J Biochem 130, 637–647 (2001)

On the Ligands in Charge-Transfer Complexes of Porcine Kidney Flavoenzyme D-Amino Acid Oxidase in Three Redox States: A Resonance Raman Study[1]

Yasuzo Nishina,*[,2] Kyosuke Sato,* Ruiwen Shi,* Chiaki Setoyama,† Retsu Miura,† and Kiyoshi Shiga*

*Departments of *Physiology and †Biochemistry, Kumamoto University School of Medicine, 2-2-1 Honjo, Kumamoto 860-0811*

Received July 25, 2001, accepted August 27, 2001

To investigate the structural modulation of ligands and their interaction in the active-site nanospace when they form charge-transfer (CT) complexes with D-amino acid oxidase (DAO) in three redox states, we compared Raman bands of the ligands in complex with DAO with those of ligands free in solution. Isotope-labeled ligands were synthesized for assignments of observed bands. The COO^- stretching of ligands observed around, 1,370 cm^{-1} downshifted by about 17 cm^{-1} upon complexation with oxidized, semiquinoid and reduced DAO, except for the case of reduced DAO-*N*-methylisonicotinate complex (8 cm^{-1} downward shift); the interaction mode of the carboxylate group with the guanidino group of Arg283 and the hydroxy moiety of Tyr228 of DAO is similar in the three redox states. The C=N stretching mode (1,704 cm^{-1}) of Δ^1-piperideine-2-carboxylate (D1PC) downshifted to 1,675 and 1,681 cm^{-1} upon complexation with reduced and semiquinoid DAO, respectively. The downward shifts indicate that the C=N bond is weakened upon the complexation. This is probably due mainly to charge-transfer (CT) interaction between D1PC and semiquinoid or reduced flavin, *i.e.*, the partial electron donation from the highest occupied molecular orbital (HOMO) of reduced flavin or a singly occupied molecular orbital (SOMO) of semiquinoid flavin to the lowest unoccupied molecular orbital (LUMO), an antibonding orbital, of D1PC. This speculation was supported by the finding that the magnitude of the shift is smaller by 5 cm^{-1} (observed at 1,680 cm^{-1}) in the case of reduced DAO reconstituted with 7,8-Cl_2-FAD, whose reduced form has lower electron-donating ability than natural reduced FAD. The amount of electron flow was estimated by applying the theory of Friedrich and Person [(1966) *J. Chem. Phys.* 44, 2166–2170] to these complexes; the amounts of charge transfer from reduced FAD and reduced 7,8-Cl_2-FAD to D1PC were estimated to be about 10 and 8% of one electron, respectively, in the CT complexes of reduced DAO with D1PC.

Key words: charge-transfer complex, D-amino acid oxidase, enzyme-ligand interaction, flavoenzyme, Raman spectra.

Except when radiation participates, all biological activities involve contact interactions between constituents (*1*). In enzyme reactions, specific interactions between enzyme and substrate take place during the course of the reaction. The interactions are responsible for the substrate recognition/specificity and the remarkable acceleration of the reaction. Thus, information about the interactions, *e.g.*, the origin and strength of the interacting force, is essential for elucidation of the molecular mechanism of the catalytic reaction.

Porcine kidney D-amino acid oxidase [D-amino acid:O_2 oxidoreductase (deaminating), EC 1.4.3.3] (DAO), which has FAD as the prosthetic group, is one of the most extensively investigated flavoenzymes. DAO catalyzes the dehydrogenation of the substrate D-amino acid to the corresponding ketimino acid; and the ketimino acid is spontaneously hydrolyzed to 2-ketoacid and ammonia. From the three-dimensional structure of DAO-ligand complexes (*2–5*), several reaction mechanisms for the reductive-half reaction of DAO have been proposed (*3, 4*): (i) the electron-proton-electron transfer mechanism (*4*), (ii) the ionic mechanism (*4*), and (iii) the hydride transfer mechanism of the α-hydrogen (*3*). However, which mechanism operates has not yet been established. In addition to the three-dimensional structure, information about the interaction of substrate/ligand with DAO in three redox states is valuable for inves-

[1] Preliminary reports of this work were presented at the Twelfth and Thirteenth Symposium on Flavins and Flavoproteins, 1996 (in Calgary, Canada) and 1999 (in Konstanz, Germany), respectively

[2] To whom correspondence should be addressed E-mail nishina@medic.kumamoto-u.ac.jp

Abbreviations AECK, aminoethylcysteine-ketimine; CT complex, charge-transfer complex, DAO, D-amino acid oxidase, HOMO, highest occupied molecular orbital, DPC, Δ^1- or Δ^2-piperideine-2-carboxylate, D1PC, Δ^1-piperideine-2-carboxylate; D2PC, Δ^2-piperideine-2-carboxylate; LAO, L-amino acid oxidase; LUMO, lowest unoccupied molecular orbital, NMIN, *N*-methylisonicotinate; OAB, *o*-aminobenzoate; RR spectra, resonance Raman spectra, SOMO, singly occupied molecular orbital.

tigation of the molecular mechanism, DAO can exist in three redox states (Scheme 1), *i.e.*, oxidized, semiquinoid (one-electron reduced), and reduced (two-electron reduced) states, and CT complexes of DAO in the three redox states are known. Each complex is a very useful model for the investigation of the catalytic mechanism; the complex of oxidized DAO is a model of an ES complex for the forward reaction, the complex of semiquinoid DAO is a model of an intermediate in the pathway of the electron-proton-electron mechanism, and the complex of reduced DAO (purple intermediate) is equivalent to an ES complex in the reverse reaction.

Recently, we reported a study of the substrate recognition and activation mechanism of DAO by spectrophotometric and thermodynamical analyses using substrate analogs, and discussed electrostatic, steric, and charge-transfer (CT) interactions as factors that affect the affinity of substrate/ligand for DAO in three redox states (*7*). It is of obvious interest to investigate in more detail the nature of the interaction between substrate/ligand and the active site, because the interaction should be truly responsible for the catalytic reaction. The purpose of the present study is to discuss the interactions qualitatively and quantitatively, based on the results of resonance Raman (RR) spectroscopy.

Vibrational spectroscopy is a useful method for studying molecular interactions as well as structural details. The vibration frequency obtained is a measure of the force constant between the atoms constituting a bond, and the constants are related to bond orders and electronic distributions between these atoms. RR spectroscopy is a practical tool for observing selectively the vibrational bands of the chromophoric groups of biomolecules. We have employed this method to determine the structures of CT complexes of flavoenzymes and the interactions among flavin, apoenzyme, and substrate/ligand in the active-site nanospace. The following information about CT complexes of DAO has been obtained. (i) In the RR spectrum of the oxidized DAO-*o*-aminobenzoate (OAB) complex excited at the CT absorption band, Raman bands at 1,583 and 568 cm^{-1}, derived from flavin and OAB, respectively, were observed. This result shows that the CT band is induced by the direct interaction between oxidized flavin and OAB (*8*), (ii) RR spectra with excitation at 632.8 nm of the anionic semiquinoid DAO complex formed in the presence of pyruvate and methylamine indicate that the complex consists of the anionic semiquinoid DAO and the zwitterionic form of *N*-methyl-α-iminopropionate produced from pyruvate and methylamine (*9*), (iii) The purple intermediate of DAO produced in its reaction with the substrate comprises a CT complex between anionic reduced flavin and the zwitterionic form of ketimino acid (*10–14*).

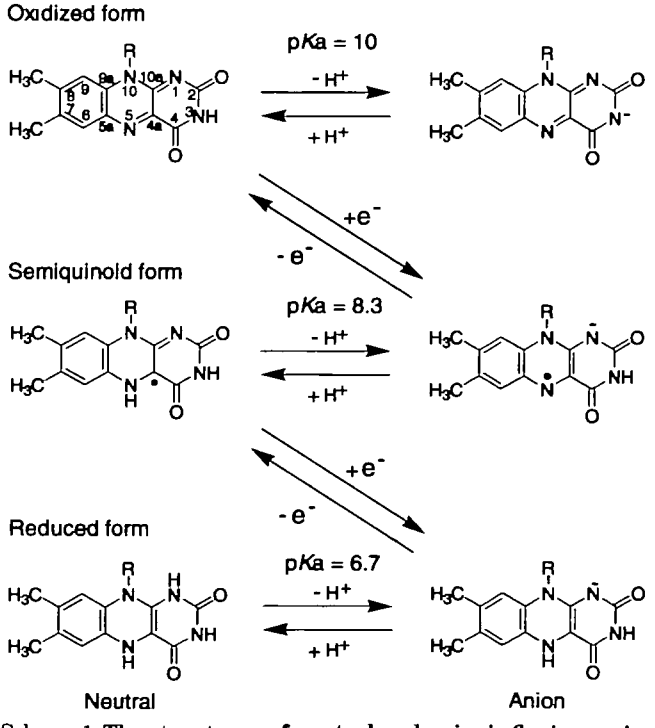

Scheme 1 **The structures of neutral and anionic flavin species in the three redox states.** Modified from Müller (*6*)

Comparison of the vibrational spectra of a substrate/ligand bound in an active-site nanospace with the spectra of the same species free in solution is expected to yield information not only on the structure but also on the electron distribution in substrate functional groups and on the molecular interaction between the substrate/ligand and the active site We have measured the RR spectra of enoyl-CoA bound to reduced acyl-CoA dehydrogenase and free in solution, and showed that the C(1)=O moiety of enoyl-CoA is strongly polarized by hydrogen bonding at the C(1)=O and that the hydrogen bonding is important for acceleration of the reaction (*15*).

In the present article, we focused on the Raman bands of ligands, and compared the bands of the ligand bound to DAO and free in solution, in order to elucidate the structural modulation and the interaction of substrate/ligand in the active-site nanospace. Isotope-labeled ligands were synthesized for assignments of the bands observed. Quantitative data on the CT interaction in CT complexes of DAO are scarce. We therefore estimated the magnitude of electron flow between flavin and ligand in CT complexes of DAO, by applying the theory about frequency shift of stretching vibration in CT complexes (*16*) to the CT complexes of DAO.

MATERIALS AND METHODS

1. Enzymes—Porcine kidney D-amino acid oxidase was purified as described elsewhere (*17–19*). Benzoate was removed from the holoenzyme purified in the form of its benzoate complex by the method reported previously (*20*). The concentrations of natural DAO and DAO reconstituted with 7,8-Cl_2-FAD were determined spectrophotometrically, using the molar absorption coefficient of 11,300 M^{-1} cm^{-1} at 455 nm and 9,500 M^{-1} cm^{-1} at 460 nm (*21*), respectively. L-Amino acid oxidase (LAO) and catalase were purchased from Sigma, USA.

2. Chemicals—[α-^{13}C]Toluene (99 atom%), *ca.* 15 M [^{15}N]-nitric acid (99 atom%), sodium [1-^{13}C]-, [2-^{13}C]-, or [3-^{13}C]-pyruvate (99 atom%), DL-[1-^{13}C]- and DL-[2-^{13}C]lysine 2HCl (99 atom%), and DL-[ε-^{15}N]lysine 2HCl (99 atom%) were purchased from Isotec, USA. Other chemicals were of highest grade available from commercial sources and used without further purification.

OAB: To obtain [carboxyl-^{13}C]- and [^{15}N]OAB (I), [α-^{13}C]-toluene and [^{15}N]nitric acid were used as starting materi-

als, respectively. A mixture of 1 4 g of concentrated H_2SO_4 and 1 0 g of 15 M HNO_3 was slowly added with vigorously stirring to 2 g of toluene at 20–25°C. The reaction mixture was kept at 25°C for 5 min and then at 30°C for 15 min. Then ice was added, and the reaction mixture was neutralized with solid Na_2CO_3. The mixture was extracted with CH_2Cl_2, and the CH_2Cl_2 phase was dried over Na_2SO_4 and evaporated to dryness. The oily product was taken up in petroleum ether (bp. 30–60°C) and applied to a silica gel 60 (130–270 mesh, Nacalai Tesque, Kyoto) column (1.5 × 20 cm). After washing the column with petroleum ether, *o*-nitrotoluene and *p*-nitrotoluene were eluted with petroleum ether containing 1% (w/w) ethyl ether. *o*-Nitrotoluene was eluted faster than *p*-nitrotoluene. The purity of the two components was monitored by thin-layer chromatography on a silica gel plate (Silicagel $70F_{254}$ plate, Wako Pure Chemical, Osaka) with petroleum ether containing 1% (w/w) ethyl ether as the mobile phase. *o*-Nitrotoluene was converted into *o*-nitrobenzoate by refluxing for 3 h in 15 ml of H_2O containing $KMnO_4$ (1 g). Excess $KMnO_4$ was reduced by H_2O_2. The filtrate collected under hot conditions was concentrated to a volume of *ca.* 2 ml by evaporation, and crystals were deposited by addition of concentrated HCl and washed with cold H_2O. *o*-Nitrobenzoic acid was reduced to OAB in 12 ml of methanol with H_2 at 100 atm and 90°C for 2 h in the presence of Raney's nickel catalyst prepared from 1.5 g of the alloy (50%). The catalyst was removed by filtration, and the filtrate was evaporated. The product (OAB) was extracted twice with CH_2Cl_2, and the CH_2Cl_2 phase was dried over Na_2SO_4, evaporated to dryness in a rotary evaporator, and left overnight in a vacuum desiccator over NaOH pellets.

AECK: Non-labeled aminoethylcysteine-ketimine (AECK) (II) was prepared from bromopyruvic acid and cysteamine in glacial acetic acid by the method of Cavallini *et al.* (*22*). ^{13}C-labeled AECK was prepared from ^{13}C-labeled bromopyruvic acid and cysteamine by the same method. The concentration of AECK was determined spectrophotometrically, using the molar absorption coefficient of 6,200 M^{-1} cm^{-1} at 296 nm (*22*). ^{13}C-labeled bromopyruvic acid was synthesized from ^{13}C-labeled sodium pyruvate by the method of Busch *et al.* (*23*) with some modification. Firstly, ^{13}C-labeled sodium pyruvate was transformed into pyruvic acid by acidifying it with hydrochloric acid and extracting with ether The resultant pyruvic acid was dried at 20°C/3 mmHg for 20 min. Bromine, dried over concentrated sulfuric acid, was gradually added with stirring to the dried pyruvic acid. A drop of concentrated sulfuric acid (5 μl) was added to the reaction mixture as a catalyst. The reaction was carried out at room temperature (*ca.* 28°C) for 2 h, then at 50°C for 1 h. The reaction products were left overnight in a vacuum desiccator over NaOH pellets and purified by re-crystallization from chloroform.

D1PC· Non-labeled and isotope-labeled Δ^1-piperideine-2-carboxylates (D1PC) (VI) were synthesized enzymatically by oxidation of non-labeled and isotope-labeled DL-lysine by DAO and LAO. DL-Lysine 2HCl (80 mg) was dissolved in 20 mM sodium pyrophosphate buffer (pH 8.3, 12 ml) and adjusted to pH 10.0 with a small volume of 1 M NaOH: the catalytic activity is strongly inhibited by the product at pH 8.3 (*24*). DAO (2 mg), LAO (4 mg), and catalase (*ca.* 1,000 units) were added to the solution and the reaction was continued under aerobic conditions for 7 h at room temperature (about 25°C). D1PC was isolated by the method of Chang *et al.* (*25*).

7,8-Cl_2-FAD: 7,8-Cl_2-Riboflavin was prepared by the method of Kuhn *et al.* (*26*) with some modification. A suspension of 4,5-dichloro-2-nitroaniline (0.1 g) and D-ribose (940 mg) in methanol (3 ml) was refluxed for 2 h. The reaction product was reduced with H_2 in an autoclave (80 atm, 60°C, 1 h) in the presence of Raney's nickel catalyst prepared from the alloy (50%, 1.5 g). After removing the catalyst by filtration, the solvent was removed under reduced pressure. The remaining syrup was immediately reacted with alloxane (100 mg) in acetic acid containing boric acid (30 mg), and the mixture was refluxed for 2 h. The precipitated crystals were collected by filtration and washed with ethanol. A part (10 mg) of crude product (40 mg) obtained was applied to a column of alumina. A yellow portion was applied to a C_{18} reverse-phase column (Nacalai Tesque, $15C_{18}$, 20 × 250 mm) and purified with a linear gradient of mobile phase (5 mM ammonium acetate, pH 5 3 to methanol). The flavin was stored as lyophilized powder. 7,8-Cl_2-FAD was prepared from the corresponding riboflavin as described previously (*11*)

3 Spectrophotometric Measurements—Visible absorption spectra were measured with a Hitachi U-3210 or U-3310 spectrophotometer thermostated at 25°C Raman spectra were obtained with a JASCO NR-1800 spectrometer (Japan Spectroscopic) with a He-Ne laser (NEC GLG 5900) or an Ar ion laser (INNOVA 70-2) as a light source. The wave number axis of the Raman spectra was calibrated for indene. RR spectra were measured in 50 mM sodium pyrophosphate or potassium phosphate buffer at room temperature (*ca.* 25°C).

4. Vibrational Analysis—Vibrational frequency calculations were carried out using the Gaussian 98 package (*27*) running on Microsoft Windows Me. The geometry of each molecule was optimized, and then Raman activities were calculated by the Hartree-Fock (HF) method with 6-31G(d) basis set. The calculated frequencies were converted by a single scaling factor of 0.8929 (*28*).

RESULTS

DAO in three redox states forms CT complexes with suitable ligands. The absorption spectra of oxidized DAO and the complexes of oxidized DAO with OAB (I) and AECK (II) are shown in Fig. 1; the spectrum of DAO-AECK complex is identical to that reported previously (*29*). The spectra of complexes of DAO in three redox states with Δ^1- or Δ^2-piperideine-2-carboxylate (DPC) are shown in Fig. 2; the ligand is Δ^2-piperideine-2-carboxylate (D2PC) (IV) with the oxidized DAO (*29*) and Δ^1-piperideine-2-carboxylate (D1PC) (VI) with the reduced (*13*) or semiquinoid (present study) DAO (see below). The spectrum of the complex of semiquinoid DAO (Fig. 2, spectrum c) was reported in this paper for the first time. Other spectra were identical with those reported previously (*24*).

1. Oxidized DAO—OAB: In the RR spectrum of oxidized DAO-OAB complex with excitation at 632.8 nm within the CT absorption band, Raman bands at 1,583 and 568 cm^{-1} derived from oxidized flavin and OAB, respectively, were observed (*8*). From these results, we concluded the CT absorption band is induced by the direct interaction between oxidized flavin and OAB, and suggested that OAB

lies along the N(5)-C(4*a*) bond and parallel to the flavin face (*8*); the positioning was confirmed by X-ray crystallography (*4*). To obtain further information on the complex, more detailed RR spectra (Fig. 3) of the complex and Raman spectra (Fig. 4) of non-labeled and isotope-labeled OAB free in solution were measured.

The 1,709-cm^{-1} band of the complex (Fig. 3A, spectrum a) is derived from the carbonyl C(4)=O stretching of FAD (*31*) The 1,617-cm^{-1} band is due to the ring stretching of OAB, but not the ring stretching of the *o*-xylene moiety of FAD, because the corresponding ring stretching band of FAD in DAO-OAB complex is observed at 1,625 cm^{-1} with excitation at 514.5 nm (*8*). The 1,583- and 1,544-cm^{-1} bands are considered to be associated with the C(4*a*)=N(5) moiety of FAD, on the basis of their similarity to the corresponding bands of the DAO-D2PC complex (*13, 30*). The 815- and 570-cm^{-1} bands are probably a ring breathing and a ring deformation of OAB, respectively; the corresponding bands of OAB free in solution are at 810 and 569 cm^{-1}, respectively.

As shown in Fig. 3B, the band intensity around 1,366 cm^{-1} decreased in the complex with [carboxyl-^{13}C]OAB, and was not influenced with [^{15}N]OAB. The difference spectrum

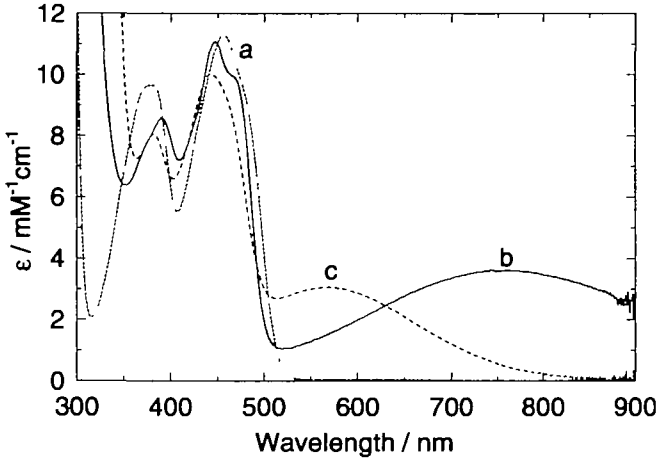

Fig 1. **Absorption spectra of complexes of DAO with OAB and AECK.** Spectra were observed in 50 mM sodium pyrophosphate buffer, pH 8 3, at 25°C. The concentrations were (a) DAO (59 μM), (b) DAO (59 μM), OAB (1 mM); (c) DAO (56 μM), AECK (0 29 mM)

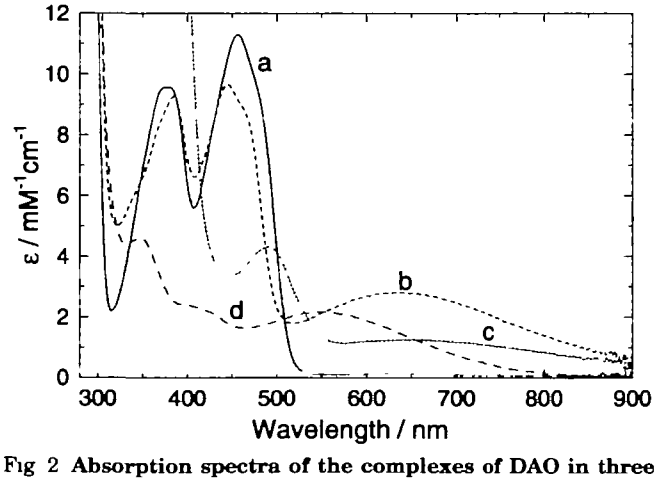

Fig 2 **Absorption spectra of the complexes of DAO in three redox states.** Spectra were recorded in 50 mM sodium pyrophosphate buffer, pH 8.3, at 25°C (a) DAO (57 μM); (b) DAO (55 μM) plus D1PC (10 mM), (c) after the addition of sodium dithionite (14 mM) to DAO (54 μM) solution containing D1PC (10 mM), (d) after the addition of D-pipecolate (10 mM) into DAO (55 μM)

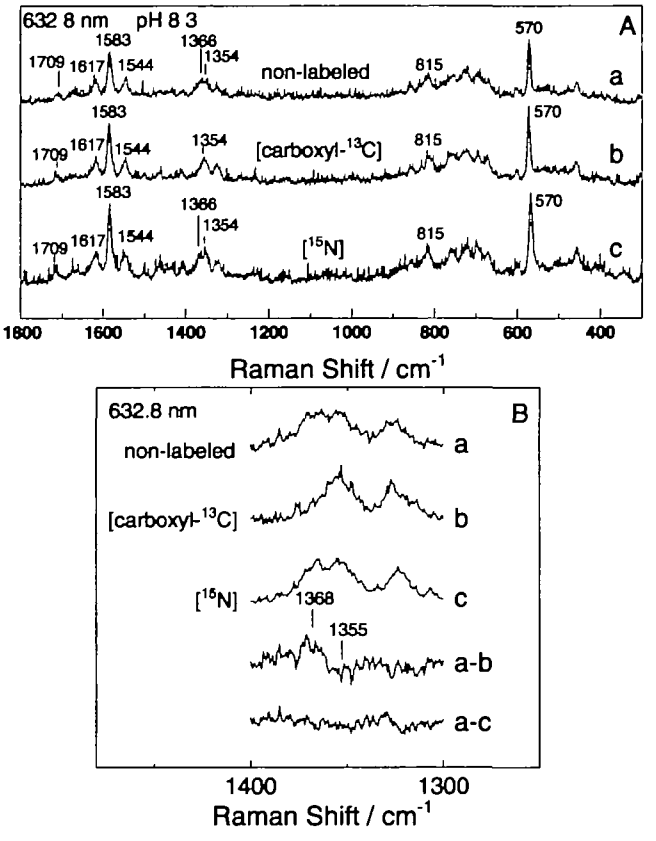

Fig. 3 **(A) Resonance Raman spectra excited at 632.8 nm of the complexes of oxidized DAO with non-labeled and isotopically labeled OAB.** The spectra were recorded in 50 mM sodium phosphate buffer, pH 8.3. The concentrations were (a) DAO (*ca* 0 7 mM), OAB (2 mM), (b) DAO (*ca.* 0.7 mM), [carboxyl-^{13}C]OAB (2 mM), (c) DAO (*ca.* 0 7 mM), [^{15}N]OAB (2 mM) **(B) Difference spectra.** The conditions for (a), (b), and (c) are the same as (A). (a–b) and (a–c) represent the difference spectra.

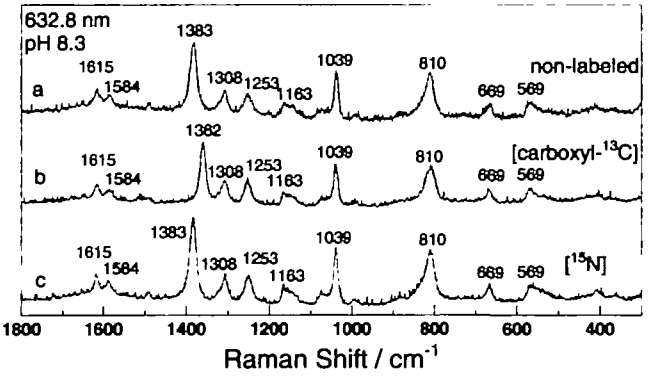

Fig. 4 **Raman spectra excited at 632.8 nm of non-labeled and isotopically labeled OAB.** Spectra were observed in sodium pyrophosphate buffer, pH 8 3 The concentrations were *ca* 300 mM (a) OAB, (b) [carboxyl-^{13}C]OAB, (c) [^{15}N]OAB

(a–b) shows that the 1,368-cm^{-1} band shifts to 1,355 cm^{-1} upon [carboxyl-^{13}C]-labeling. The 1,383-cm^{-1} band of OAB free in solution (Fig. 4) shifted to 1,362 cm^{-1} upon [carboxyl-^{13}C]-labeling. The bands associated with C=O stretching of the COOH and COO^- symmetric stretching of carboxylate appear around 1,700 cm^{-1} and in the 1,340–1,440 cm^{-1} region, respectively (*32*). Thus, the 1,368-cm^{-1} band in the complexed state and the 1,383-cm^{-1} band in the free state are clearly assigned to the COO^- symmetric stretching, but not to COOH.

This indicates that the carboxylate group of OAB remains unprotonated when it binds to DAO. The band-shift from 1,383-cm^{-1} to 1,368 cm^{-1} (15 cm^{-1} downward shift) shows that the bond strength of the carboxyl group in OAB is weakened by the complexation.

AECK: Raman spectra of non-labeled and ^{13}C-labeled AECK (II) free in solution are shown in Fig 5 The 1,622-cm^{-1} band shifted to 1,607 cm^{-1} and 1,587 cm^{-1} upon [2-^{13}C]- and [3-^{13}C]-labeling, respectively; only a small shift occurred upon [carboxyl-^{13}C]-labeling. The 1,379-cm^{-1} band shifted to 1,355 cm^{-1} upon [carboxyl-^{13}C] labeling. These indicate that the 1,622- and 1,379-cm^{-1} bands are C(2)=C(3) stretching and COO^- symmetric stretching, respectively, because the bands for C(2)-C(3) single bond and for COOH should be found around 1,000 and around 1,700 cm^{-1}, respectively. Therefore, AECK is in the enaminic form, not in the ketiminic form (Chart 1), and this is consistent with the results of NMR study by Cavallini *et al.* (*22*).

The RR spectra of the complex of DAO with non-labeled and ^{13}C-labeled AECK excited at 632.8 nm within the CT absorption band are shown in Fig. 6. The carboxylate group of AECK remains unprotonated when it binds to DAO This is shown by the 1,362-cm^{-1} band observed in the complex. The 1,606-cm^{-1} band is derived from C(2)=C(3) stretching of AECK, because the band disappeared upon [2-^{13}C]-labeling (the band probably shifts to low frequency and is concealed behind the 1,578-cm^{-1} band) and shifted to 1,568 cm^{-1} upon [3-^{13}C]-labeling. The 1,578- and 1,544-cm^{-1} bands (Fig 6) observed in DAO-AECK complex are typical of flavin bands and correspond to those (1,583- and 1,544-cm^{-1} bands) observed in the DAO-OAB complex Namely, the resonance-enhanced Raman bands obtained are from FAD and AECK. Therefore, the CT interaction occurs between FAD and AECK. The bonds of the C(2)=C(3) and C-O of COO^- in AECK are weakened by the complex formation, since the 1,622- and 1,379-cm^{-1} bands of AECK shifted to 1,606 cm^{-1} (16 cm^{-1} downward shift) and 1,362 (17 cm^{-1} downward shift), respectively.

2. Semiquinoid and Reduced DAO—The visible absorption spectrum (Fig. 2, spectrum c) was observed after the addition of dithionite to oxidized DAO solution containing D1PC, and the spectrum did not change for hours; the spectrum is characteristic of an anionic flavosemiquinone (an absorption peak around 480 nm). Previously, we reported from RR studies that the ligand bound to oxidized DAO is D2PC (IV) (*30*), and the ligand bound to reduced DAO is D1PC (VI) in zwitterionic form (*13*). The ligand bound to semiquinoid DAO (Fig. 2, spectrum c) is zwitterionic D1PC as described below.

In contrast to AECK, DPC in solution is mainly in the ketiminic form (V), not in the enaminic form (IV). Raman

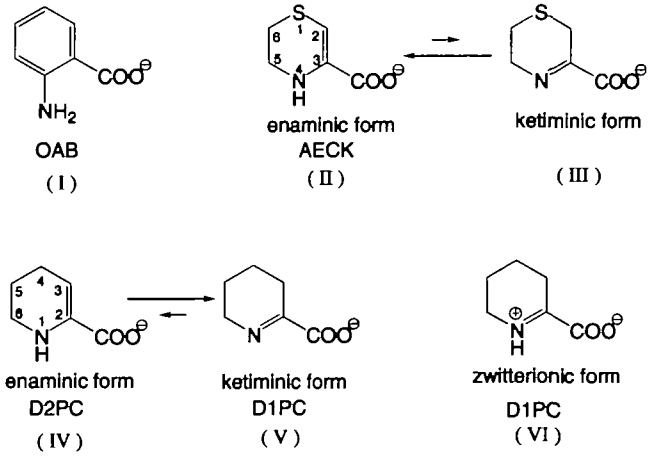

Chart 1. **Structures of ligands.**

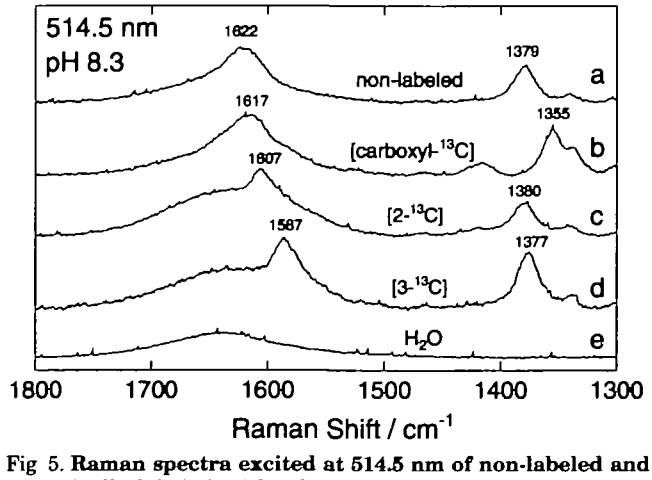

Fig 5. **Raman spectra excited at 514.5 nm of non-labeled and isotopically labeled AECK.** Spectra were recorded in sodium pyrophosphate buffer. The concentrations were (a) AECK (35 mM), pH 8.3, (b) [carboxyl-^{12}C]AECK (60 mM), pH 8.3, (c) [2-^{13}C]AECK (18 mM), pH 8.4; (d) [3-^{13}C]AECK (32 mM), pH 8.4, (e) H_2O.

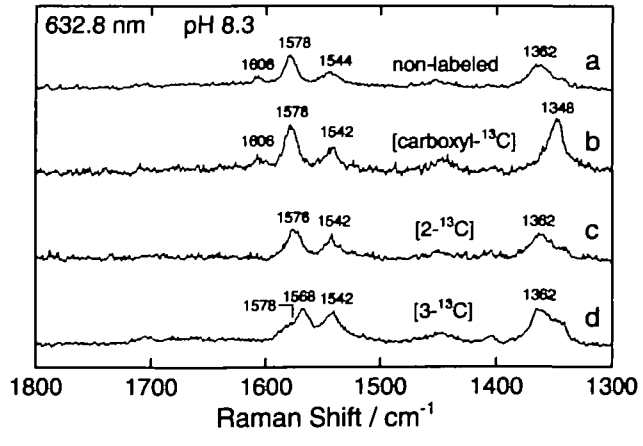

Fig 6 **Resonance Raman spectra excited at 632.8 nm of the complexes of DAO with non-labeled and isotopically labeled AECK.** Spectra were recorded in 50 mM sodium pyrophosphate buffer, pH 8 3. The concentrations were: (a) DAO (1.1 mM), AECK (1.1 mM), (b) DAO (1 3 mM), [carboxyl-^{13}C]AECK (1 3 mM), (c) DAO (0 9 mM), [2-^{13}C]AECK (0.9 mM), (d) DAO (1.4 mM), [3-^{13}C]AECK (1.4 mM).

spectra of non-labeled and isotope-labeled D1PC in solution are shown in Fig. 7. As the pK_a value of D1PC at the N atom is 8.0 (*13*), D1PC is in zwitterionic form at pH 6.0. The 1,704-cm^{-1} band (Fig. 7, spectrum a) is assigned to the C=N stretching mode. This can be seen from its 24-cm^{-1} and 34-cm^{-1} downward shifts upon [^{15}N]- and [2-^{13}C]-labeling, respectively (Fig. 7, spectra b and d). The COO^- stretching mode splitting into two components at 1,387 and 1,352 cm^{-1} is assigned to a coupling with CH_2 deformation of C(3)H_2. Both the 1,387- and 1,352-cm^{-1} bands changed in D_2O at pD 6.0 (Fig. 7, spectrum e). The cause of this change is probably the exchange of hydrogen at the C(3) by deuterium; the ketimine-enamine equilibrium (IV, V) is responsible for the exchange (H to D).

The RR spectra of the complexes of reduced DAO with D1PC have already been reported (*13*). The RR spectra of the complexes of semiquinoid DAO with DPC are shown in Fig. 8, together with those of the complex of reduced DAO with D1PC for comparison (Fig. 8, spectra a and d). The 1,681-cm^{-1} band (Fig. 8, spectrum b) is assigned to C=N stretching vibration of D1PC (VI) based on the 16-cm^{-1} downward shift (1,665 cm^{-1}) (Fig. 8, spectrum c) upon [^{15}N]-labeling. The corresponding band in the complex of reduced DAO is observed at 1,675 cm^{-1} (Fig. 8, spectrum a); the band has been assigned to be a C=N stretching of D1PC

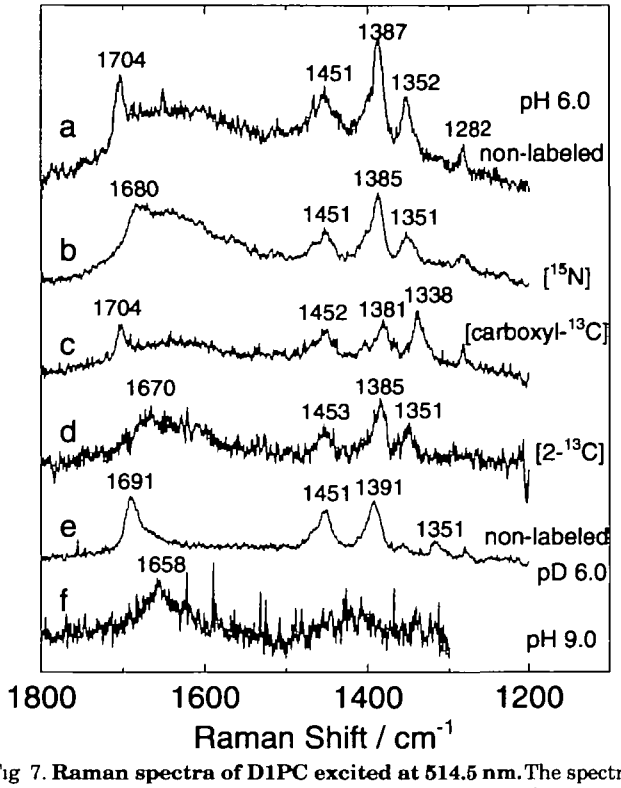

Fig 7. **Raman spectra of D1PC excited at 514.5 nm.** The spectra were recorded in 50 mM sodium phosphate buffer in H_2O and D_2O The concentration of D1PC was about 300 mM

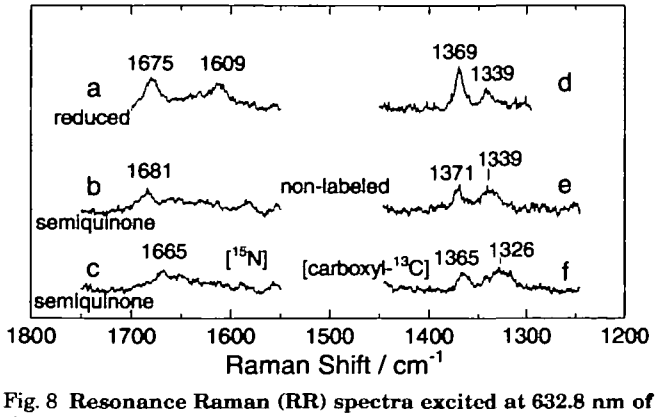

Fig. 8 **Resonance Raman (RR) spectra excited at 632.8 nm of the complexes between reduced or semiquinoid DAO and D1PC.** Spectra were recorded in 50 mM sodium pyrophosphate buffer, pH 8.3. The concentrations were: (a) DAO (*ca* 0 8 mM), D-pipecolate (63 mM); (b) DAO (*ca*. 1 mM), D1PC (150 mM), dithionite (16 mM); (c) DAO (*ca* 1 mM), [^{15}N]D1PC (150 mM), dithionite (32 mM); (d) DAO (*ca*. 1 mM), D-pipecolate (70 mM); (e) DAO (*ca* 1 mM), D1PC (108 mM), dithionite (22 mM); (f) DAO (*ca* 1 mM), [carboxyl-^{13}C]D1PC (110 mM), dithionite (22 mM).

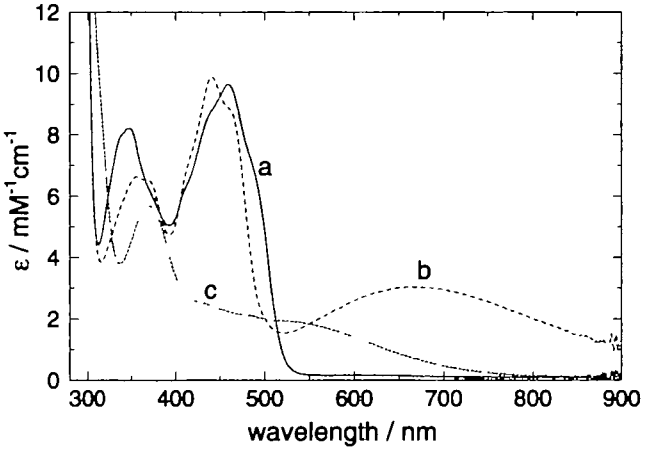

Fig 9 **Absorption spectra of DAO reconstituted with 7,8-Cl_2-FAD.** Spectra were recorded in 50 mM sodium pyrophosphate buffer, pH 8 3, at 25°C The concentrations were (a) DAO (61 μM), (b) DAO (60 μM), D1PC (2 2 mM), (c) DAO (60 μM), D-proline (9 9 mM).

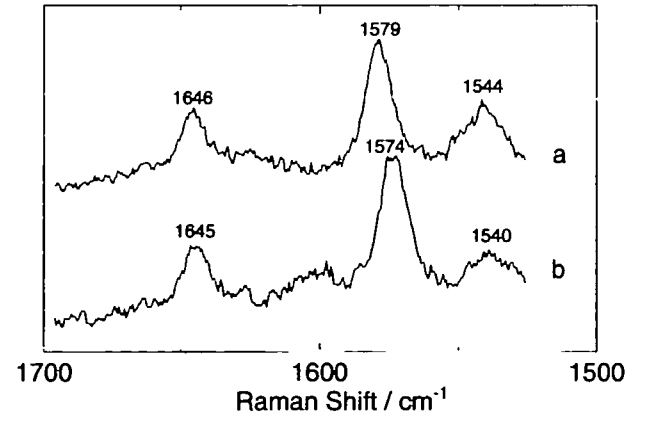

Fig. 10. **Resonance Raman spectra excited at 632.8 nm of the complexes of D2PC with DAO and DAO reconstituted with 7,8-Cl_2-FAD.** Spectra were recorded in 50 mM sodium phosphate buffer, pH 8 3. The concentrations were (a) DAO (*ca*. 1 mM), DPC (3 mM); (b) DAO reconstituted with 7,8-Cl_2-FAD (*ca*. 0 8 mM), DPC (3 mM)

(VI) by isotope effects (*13*). The frequency is lower than that of the complex with semiquinoid DAO. The 1,371- and 1,339-cm^{-1} bands are associated with the COO^- stretching mode, judging from the downward shifts upon [carboxyl-^{13}C]-labeling (Fig. 8, spectra e and f). The broad 1,339-cm^{-1} band (Fig. 8, spectrum e) probably contains a band of anionic semiquinoid flavin [the 1,331-cm^{-1} band has been observed in semiquinoid DAO-ligand complex (*33*)], thus the band position and the amount of the isotope shift involve some ambiguity. Nevertheless, the ligand is obviously in the ketiminic form in the complex of semiquinoid DAO. Previously, the calculation of HOMO and LUMO of some emaminic and ketiminic forms by the extended Huckel molecular orbital method indicated that the enaminic form is a better electron donor than the ketiminic form, and the ketiminic form is a better electron acceptor than the enaminic form (*34*). Thus, in the CT complex of semiquinoid DAO, D1PC acts as an electron acceptor as well as in the case of the CT complex of reduced DAO, and the D1PC is in the zwitterionic form (VI), because ligands capable of binding to reduced or anionic semiquinoid DAO are in a zwitterionic form (*6, 9, 35, 36*).

3. DAO Reconstituted with 7,8-Cl_2-FAD—The introduction of electronegative groups into the xylene moiety of the isoalloxazine ring affects the CT interaction between flavin and ligand. The substitution with electronegative chlorine strengthens the ability of oxidized flavin to accept electrons and weakens the ability of reduced flavin to donate electrons. Actually, in the case of DAO reconstituted with 7,8-Cl_2-FAD, CT absorption band of the complex of the oxidized DAO with D2PC shifts to longer wavelength (Fig 9, spectrum b), and the band of the complex of the reduced DAO with D1PC to shorter wavelength (Fig. 9, spectrum c) A similar red shift has been reported in the complex of the oxidized DAO with OAB (*21*). To investigate the shift of Raman bands caused by CT interaction, we measured RR spectra of the complexes of DAO reconstituted with 7,8-Cl_2-FAD. In the case of oxidized DAO, the C(2)=C(3) stretching (1,646 cm^{-1}) of D2PC (IV) is lower by merely 1 cm^{-1} in the case of the reconstituted DAO complex than in the case of natural DAO (Fig. 10). On the other hand, in the case of reduced DAO, the 1,675-cm^{-1} band of C=N stretching of D1PC (VI) is higher by 5 cm^{-1} in the case of the reconstituted DAO than in the case of natural DAO (Fig. 11, spectra a and b). Similar results were obtained for the purple complex of DAO with D-proline (CT complex of reduced DAO with Δ^1-pyrrolidine-2-carboxylate) (Fig. 11, spectra c and d); the band of C=N stretching of the ligand was obtained at 1,658 and 1,664 cm^{-1} for the natural and reconstituted DAO, respectively. The 1,609- and 1,605-cm^{-1} bands observed in natural enzyme (Fig. 11, spectra a and c) are for the C(4a)=C(10a) stretching vibrational mode (*7*). The corresponding band in the reconstituted DAO is not clear. The band associated with COO^- was scarcely affected in the complex with D1PC and upshifted by 5 cm^{-1} in the complex with Δ^1-pyrrolidine-2-carboxylate upon the reconstitution.

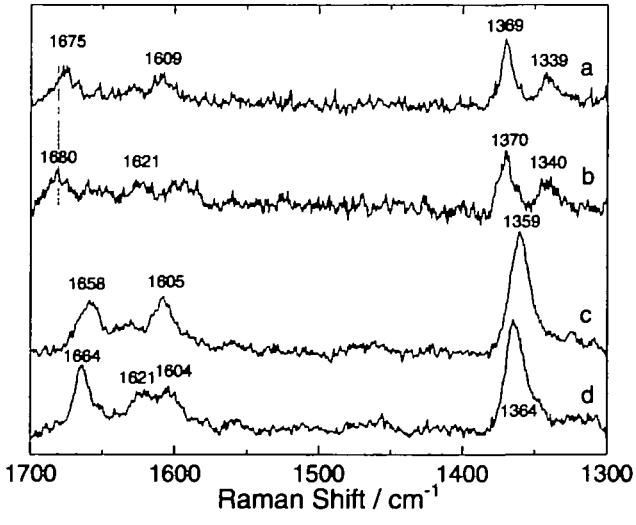

Fig 11. **Resonance Raman spectra of the complexes of reduced DAO and reduced DAO reconstituted with 7,8-Cl_2-FAD.** Spectra were recorded in 50 mM sodium phosphate buffer, pH 8 3 The concentrations were (a) DAO (*ca.* 1 mM), D-pipecolate (70 mM), (b) DAO reconstituted with 7,8-Cl_2-FAD (*ca* 1.3 mM), D-pipecolate (70 mM), (c) DAO (*ca.* 1 mM), D-proline (48 mM), (d) DAO reconstituted with 7,8-Cl_2-FAD (*ca.* 1.3 mM), D-proline (48 mM).

DISCUSSION

We investigated in this report mainly the CT complexes of DAO in three redox states and compared the spectrum of a ligand in the free state and the complexed state. Previously reported data and the present findings on COO^- stretching and the dissociation constants (K_d) between ligands and oxidized or reduced DAO are summarized in Table I. The COO^- bands for the complexed state were observed around 1,370 cm^{-1}, and the frequencies in the complex were lower than those of the ligands free in solution. This indicates that the COO^- remains unprotonated in all the complexes, and the bond is weakened compared with the free ligands Except in the case of reduced DAO-NMIN complex, the magnitude of the shift is about 17 cm^{-1}, *i.e.*, the band shift upon complexation is almost the same regardless of the redox state of DAO. This suggests that the interaction modes of the carboxylate group with the active site are similar in the three redox states. The interaction of the carboxylates of ligands with Arg283 and the hydroxy moiety of Tyr228 in oxidized and reduced states has been clearly shown by studies of crystal structure (*2–5*). As a whole, the carboxylate groups of various ligands probably behave similarly in their interaction with DAO. The exceptionally small shift in the case of reduced DAO-NMIN complex sug-

TABLE I **COO^- Raman frequencies of ligands free in solution and bound to DAO (cm^{-1}) and dissociation constants, K_d (μM).**

	Free (*m*)	Complex (*n*)	*m–n*	K_d (μM)
Oxidized DAO-AECK	1,376	1,362	17	0.33[a]
Oxidized DAO-OAB	1,383	1,368	15	20[b]
Reduced DAO-picolinate[c]	1,393	1,376	17	0 84
Reduced DAO-NMIN[d]	1,385	1,377	8	500
Reduced DAO-D1PC[e]	1,387	1,369	18	6 3[f]
	1,352	1,339	13	
Semiquinoid DAO-D1PC	1,387	1,371	16	not determined
	1,352	*ca* 1,339	*ca* 13	

[a]Value from Ricci *et al.* (*29*). [b]Value from Massey and Ganther (*37*) [c]Data from Nishina *et al.* (*35*) [d]Data from Nishina *et al.* (*7*). [e]RR data from Nishina *et al.* (*13*) [f]Unpublished result

gests that the electrostatic interaction of COO^- with the amino acid residues is weaker, although the reason is presently unknown, and the dissociation constant is consequently larger than others (Table I).

On the contrary, the interaction mode of portions other than the carboxylate group is different depending on the ligand species, that is, the C(2)=C(3) band (1,622 cm^{-1}) of AECK is largely downshifted, but the 569-cm^{-1} band of the ring deformation mode of OAB remains almost constant upon the complexation with oxidized DAO. Previously, we proposed that the CT complex of oxidized DAO has a structure with the ligand, an electron donor, lying parallel to the flavin face, which is an electron acceptor, and with the HOMO of the ligand overlapping with the LUMO of flavin (*34*) Taking this proposition into account, we conclude that the electron donation from HOMO of ligand to the LUMO of flavin, which is the antibonding orbital (*34*), may be less in the case of the OAB complex than the AECK complex. This hypothesis is supported by the fact that the Raman band of flavin of the complex is downshifted in the AECK complex (1,578 cm^{-1}) compared with that of the OAB complex (1,583 cm^{-1}). These bands are associated with the C(4*a*)=N(5) bond of flavin The difference in the interaction mode can be seen, for example, in the case of the DAO-benzoate complex, which does not show the CT interaction. Recent studies of crystal structure of DAO-ligand complexes (*2–5*) showed that the plane of benzoate or of OAB is parallel to that of flavin, but the position of benzoate is slightly closer to flavin than that of OAB. This result makes it difficult to conclude that the π-electron orbital of benzoate does not overlap with that of flavin. Therefore, the reason why the benzoate complex does not form a CT complex is probably due to the character of the ionization potential of benzoate. We conclude from the discussions above that in the interaction between DAO and ligands, the carboxylate group interacts with DAO in a similar manner, but the other portions behave differently from one another. The interaction of the carboxylate in the active-site nanospace is unequivocally important for the location of a substrate in the active site, and the substrate specificity of DAO is probably due to the interaction of the other portion.

As described here, some Raman bands of substrate/ligand were shifted by its binding into enzyme active-site nanospace. It is desirable to clarify not only information on the structural modulation of substrate/ligand, but also the molecular mechanism of the modulation, on the basis of the data of the band shifts. The forces that cause the shift of a Raman band include CT interaction, hydrogen-bonding interaction, electrostatic interaction, van der Waals force *etc*. Here, we focus on the Raman band of zwitterionic D1PC in the complexes of reduced and semiquinoid DAO. According to studies of factors affecting the C=N stretching in protonated retinal Schiff base (*38–40*), the C=N stretching frequency is pushed to higher frequency by coupling with the C=N-H bending vibration, and the frequency is shifted to lower frequency by weakening hydrogen-bonding interaction at the C=N-H moiety. However, it was recently found that the cationic protonated ketimino nitrogen is within hydrogen-bonding distance (3.0 Å) of the backbone carbonyl oxygen of Gly313 in the purple intermediate of DAO with D-proline, which is the complex of reduced DAO with Δ^1-pyrrolidine-2-carboxylate, by the X-ray structural analyses (*5*). D1PC, which is a similar ketimino acid to Δ^1-pyrrolidine-2-carboxylate, is expected to occupy a similar position in the active-site nanospace and should also have a fairly strong hydrogen-bonding interaction at the C=N-H moiety. Thus, the weakening of the hydrogen bonding cannot be responsible for the low frequency shift of the 1,704-cm^{-1} band CT interaction is also known to be an important factor in the shift of a vibrational band. CT interaction is largely dependent on the nature of both the HOMO of an electron donor and the LUMO of an electron acceptor. CT interaction is a chemical bond formed by the partial flow of an electron cloud from the HOMO of a donor molecule into the LUMO of a partner acceptor molecule. The CT interaction is strong when the overlap integral between HOMO of the electron donor and LUMO of the electron acceptor is large and the energy gap (E_{HOMO}–E_{LUMO}) between the donor HOMO and the acceptor LUMO is small. The electron donation occurs from the HOMO to the LUMO. Thus, the higher the energy of the HOMO of a compound is, the better electron donor it is, and the lower the energy of the LUMO of a compound is, the better electron acceptor it is. Previously, we calculated the HOMO and LUMO of some enaminic and ketiminic forms by the extended Huckel molecular orbital method (*34*); the enaminic form is a better electron donor than the ketiminic form and ketiminic form is a better electron acceptor than the enaminic form. The following ideas were also supported. (i) In the CT complex of oxidized DAO, the oxidized flavin is an electron acceptor and the ligand is an electron donor. (ii) In the CT complex of reduced DAO, the reduced flavin is an electron donor and the ligand is an electron acceptor. The partial flow of an electron cloud from the HOMO of reduced flavin to the LUMO of D1PC is important for CT interaction in the complex of reduced DAO with D1PC. The coefficients of atomic π orbitals in the LUMO of the ketiminic form are opposite in sign and fairly large at the C and N atoms in the C=N moiety (*34*). Thus, the low shift of the C=N band in the complex is qualitatively explained as weakening of the C=N bond by electron donation from the HOMO of reduced flavin to the LUMO, anti-bonding orbital, of the ketiminic form.

In the CT complex of semiquinoid DAO, the electron acceptor is D1PC (VI) as mentioned in "RESULTS." Thus, the electron donation from the SOMO of semiquinoid DAO to the LUMO of D1PC is important for the CT interaction. The smaller shift of C=N stretching of D1PC in the case of semiquinoid DAO than in the case of reduced DAO (Table II) suggests that the electron-donating ability of semiquinoid flavin is weaker than that of reduced flavin; a simi-

TABLE II. **C=N Raman frequencies of D1PC free in solution and bound to DAO (cm^{-1}).** In parentheses are the difference from the frequency in free state.

Free	1,704 (0)
Reduced DAO	1,675 (29)
Reduced DAO reconstituted with 7,8-Cl_2-FAD	1,680 (24)
Semiquinoid DAO	1,681 (23)

TABLE III **C=N Raman frequencies of *N*-methyl-α-iminopropionate bound to DAO (cm^{-1}).**

Reduced DAO[a]	1,671
Semiquinoid DAO[b]	1,677

[a]Raman datum from Nishina *et al.* (*13*). [b]Raman datum from Nishina *et al* (*9*).

lar difference in the frequency shift was also recognized in the case of *N*-methyl-α-iminopropionate as a ligand (Table III). In either case, the band shift of C=N stretching of D1PC (VI) by complex formation with reduced or semiquinoid DAO is largely due to the CT interaction, not to hydrogen bonding.

Friedrich and Person (*16*) referred to the following notions with regard to the vibrational bands of ligands in CT complexes. When the infrared spectra of CT complexes are compared with those of isolated molecules which form the complexes, three types of changes are found to occur: (i) the vibrational frequencies in donor or acceptor (or both) may be shifted, (ii) the intensities of the bands may be changed considerably, and (iii) new low-frequency bands appear due to the vibrations of one molecule in the complex against the other They discussed theoretically the first two changes. Here, we apply the treatment for the frequency shift of the vibrational mode of the ligand upon CT-complexation to the CT complex of D1PC (VI) with reduced DAO. When A and D represent an electron acceptor and donor molecule, respectively, a wave function which represents CT interaction can be expressed by an approximate wave function Ψ that is a linear combination of two resonance structures (*41*).

$$\Psi(\mathrm{D{\cdot}A}) = a\Psi_0(\mathrm{D, A}) + b\Psi_1(\mathrm{D^+{\cdot}A^-})$$

Here Ψ_0(D, A) and $\Psi_1(D^+{\cdot}A^-)$ represent wave functions of no-bond and dative structures, respectively. The potential for the X-Y (C=N in this case) bond is a function of distance $r_{X\text{-}Y}$. For the no-bond state, this function can be loosely approximated by the potential function for the free D1PC; in the dative state, it is given closely by the function for the free $D1PC^-$ form with one electron accepted from reduced flavin in DAO. The potential function for the X-Y bond in the complex is given approximately by

$$W_N(\mathrm{X\text{-}Y}) = (a^2 + abS)W_0(\mathrm{X\text{-}Y}) + (b^2 + abS)W_1(\mathrm{X\text{-}Y})$$

Here S represents an overlap integral between Ψ_0 and Ψ_1, the coefficients $(a^2 + abS)$ and $(b^2 + abS)$ are the weight of the no-bond and dative structures, respectively, and W_0 and W_1 represent potential functions for no-bond and dative structures, respectively. The force constant for the X-Y bond in the complex,

$$k_N \equiv (a^2 + abS)k_0 + (b^2 + abS)k_1$$

Here k_0 and k_1 are the X-Y stretching force constants in free D1PC and $D1PC^-$, respectively. Using the normalization condition $(a^2 + 2abS + b^2 = 1)$, the following equation was obtained.

$$\Delta k/k \equiv (k_0 - k_N)/k_0 = [1 - (k_1/k_0)](b^2 + abS)$$

This shows the approximate relationship between the frequency shift of the X-Y stretching and the weight of the dative state in the structure of the complex $(b^2 + abS)$. The ratio $\Delta k/k$ is given in good approximation by $2\Delta\nu/\nu \equiv 2(\nu_0 - \nu)/\nu_0 \simeq \Delta k/k$ for small frequency shift in weak complexes (*16, 40*). We must estimate the frequency for the X-Y stretch in $D1PC^-$ to obtain the ratio k_1/k_0. We estimated the frequency by using an *ab initio* molecular orbital method, because estimation based on experimental methods is difficult. The bond lengths of X-Y (C=N or C-N) in D1PC and $D1PC^-$ are 1.273 and 1.406 Å, respectively. This indicates that the C=N bond is moderately weakened when D1PC accepts one electron The frequencies mainly associated with X-Y in D1PC and $D1PC^-$ are calculated to be 1,688 cm^{-1} and 1,359 cm^{-1}, respectively. Thus, the ratio $k_1/k_0 = 0.65$. If the low frequency shift upon the complexation with reduced DAO is due to only the CT interaction, the dative structure can be approximately evaluated from the value of $b^2 + abS$, using the following equation with the value of $\Delta\nu/\nu$ experimentally obtained.

$$b^2 + abS = 5.7 \times \Delta\nu/\nu$$

The amount of the charge transferred (the amount of the dative structure) from reduced flavin to D1PC (VI) is estimated to be 9.7% of one electron, the amount in the case of DAO reconstituted with 7,8-Cl_2-FAD to be 8.0%, and the amount transferred from semiquinoid flavin to D1PC in the complex of semiquinoid DAO to be 7.7%.

Here, k_0 and k_1 are defined as the corresponding force constants in free D1PC and $D1PC^-$, respectively, but should originally be chosen as the constants in the no-bond structure and in the dative structure, respectively The magnitude of the force constants in the no-bond structure or dative structure should deviate from that in the free state as a result of electrostatic interaction, van der Waals force, *etc.* Thus, the present estimation may contain an ambiguity. However, this ambiguity can be reduced by the comparison of natural DAO and DAO reconstituted with 7,8-Cl_2-FAD; the geometrical structure of flavin, ligand, and amino acid residues in the active-site nanospace is considered to be the same in each case. The difference in electron donation of 1.7% between natural DAO and the reconstituted DAO is due to the difference in electron-donating ability of the two reduced flavins, and indicates that CT interaction is undoubtedly a large factor in the band shift

Furthermore, it is worthwhile to note the 1,574-cm^{-1} band of the complex of oxidized DAO reconstituted with 7,8-Cl_2-FAD with D2PC (Fig. 10): the band is associated with the C(4*a*)=N(5) bond of 7,8-Cl_2-FAD. Although the frequency of the corresponding band in uncomplexed 7,8-Cl_2-FAD-DAO is not known, it is considered to be positioned near the corresponding band in natural DAO, because the corresponding bands of riboflavin and 7,8-Cl_2-riboflavin bound to riboflavin binding protein were observed at the same position (1,583 cm^{-1}) (*42*); the bands for those free in solution were of similar frequency (*43*). Thus, the difference between 1,579 cm^{-1} (FAD) (Fig. 10, spectrum a) and 1,574 cm^{-1} (7,8-Cl_2-FAD) (Fig 10, spectrum b) is probably due to the difference in CT interaction; in the case of 7,8-Cl_2-FAD, which has higher electron acceptability than FAD, the electron donation from the HOMO of D1PC to the LUMO of 7,8-Cl_2-FAD, which is an antibonding molecular orbital, increases and the band shifts to lower frequency than in the case of natural DAO. In this case, A^- in the dative form is anionic flavosemiquinone. The band associated with C(4*a*)=N(5) stretching of anionic flavosemiquinone of DAO has been observed at 1,331 cm^{-1} (*33*). Thus, we assumed the frequencies of the corresponding bands in the no-bond and dative structures are 1,583 and 1,331 cm^{-1}, respectively, and also estimated the electron flow from D2PC to oxidized flavin by the same procedure mentioned above. The magnitudes were estimated to be 1.7 and 3.8% for the natural and the 7,8-Cl_2-FAD–reconstituted enzymes, respectively; the electron flow is *ca.* 2% larger in 7,8-Cl_2-FAD-DAO than in natural DAO

The X-ray crystallographic structural analysis for both CT complexes of oxidized and reduced DAOs have been carried out and clarified the alignment between the flavin ring and a ligand. The alignments are consistent with CT interaction; the overlap between HOMO of ligand and LUMO of oxidized flavin become large in oxidized DAO (*4*), and the overlap between LUMO of ligand and HOMO of reduced flavin is large in reduced DAO (*5*). In this paper, we studied the structural modulation of ligands and the interaction thereof experienced in the active-site nanospace when they form CT complexes with DAO in three redox states by means of Raman spectroscopy. The COO^- streching of ligands observed around 1,370 cm^{-1} downshifts by about 17 cm^{-1} upon complexation with DAO, indicating that the interaction mode of the carboxyl group in the active site is similar in the three redox states. We could also estimate the magnitude of the electron flow through the overlap between HOMO and LUMO, on the basis of the frequency shift of Raman bands of ligand upon the complexation with DAO. A new bond between flavin and substrate/ligand is formed by an intermolecular delocalization of electron, and the delocalization functions toward weakening of an intramolecular bond. The delocalization leads to a change in bond along the reaction pathway and is a driving force for propulsion of a chemical reaction. HOMO-LUMO interaction is generally important for the delocalization of electron. Thus, the overlap between HOMO and LUMO, which is recognized in CT complexes of DAO, is a candidate for the pathway of electron and is probably important for redox reaction of DAO.

REFERENCES

1 Klotz, I M (1986) *Introduction to Biomolecular Energetics*, pp. 103–133, Academic Press, London
2 Mizutani, H , Miyahara, I , Hirotsu, K., Nishina, Y , Shiga, K., Setoyama, C , and Miura, R (1996) Three-dimensional structure of porcine kidney D-amino acid oxidase at 3 0 Å resolution *J Biochem.* **120**, 14–17
3. Mattevi, A., Vanoni, M.A., Todone, F , Rizzi, M , Teplyakov, A., Coda, A., Bolognesi, M , and Curti, B (1996) Crystal structure of D-amino acid oxidase. A case of active site mirror-image convergent evolution with flavocytochrome *b2* *Proc. Natl Acad Sci USA* **93**, 7496–7501
4 Miura, R , Setoyama, C., Nishina, Y., Shiga, K., Mizutani, H , Miyahara, I , and Hirotsu, K. (1997) Structural and mechanistic studies on D-amino acid oxidase-substrate complex. Implications of the crystal structure of enzyme substrate analog complex *J Biochem.* **122**, 825–833
5. Mizutani, H , Miyahara, I., Hirotsu, K., Nishina, Y , Shiga, K., Setoyama, C., and Miura, R. (2000) Three-dimensional structure of the purple intermediate of porcine kidney D-amino acid oxidase Optimization of the oxidative half-reaction through alignment of the product with reduced flavin *J Biochem* **128**, 73–81
6 Muller, F (1991) Free flavins. Synthesis, chemical and physical properties in *Chemistry and Biochemistry of Flavoproteins* (Müller, F , ed) Vol I, pp 1–71, CRC Press, Boca Raton, Florida
7. Nishina, Y., Sato, K., Miura, R , and Shiga, K. (2000) Substrate recognition and activation mechanism of D-amino acid oxidase· A study using substrate analogs. *J. Biochem.* **128**, 213–223
8 Nishina, Y , Shiga, K., Tojo, H , Miura, R , Watari, H , and Yamano, T. (1981) Resonance Raman study of D-amino acid oxidase-inhibitor complexes. *J. Biochem* **90**, 1515–1520
9. Nishina, Y , Tojo, H , Miura, R., Miyake, Y , and Shiga, K. (1988) Complex formation between anionic semiquinoid form of a flavoenzyme D-amino acid oxidase and ligands. Stabilizing mechanism of anionic semiquinoid flavoenzyme *J Biochem* **104**, 727–733
10 Nishina, Y , Shiga, K., Watari, H , Miura, R., Miyake, Y., Tojo, H , and Yamano, T (1982) Resonance Raman study on the purple intermediates of the flavoenzyme D-amino acid oxidase. *Biochem Biophys. Res. Commun.* **106**, 818–822
11 Miura, R , Nishina, Y., Ohta, M., Tojo, H , Shiga, K., Watari, H , Yamano, T , and Miyake, Y. (1983) Resonance Raman study on the flavin in the purple intermediates of D-amino acid oxidase *Biochem Biophys. Res. Commun* **111**, 588–594
12. Nishina, Y , Shiga, K., Miura, R , Tojo, H , Ohta, M , Miyake, Y , Yamano, T , and Watari, H. (1983) On the structures of flavoprotein D-amino acid oxidase purple intermediates. A resonance Raman study *J Biochem* **94**, 1979–1990
13 Nishina, Y , Miura, R , Tojo, H , Miyake, Y , Watari, H , and Shiga, K. (1986) A resonance Raman study on the structures of complexes of flavoprotein D-amino acid oxidase. *J Biochem* **99**, 329–337
14. Nishina, Y , Sato, K., Miura, R , and Shiga, K. (1998) Resonance Raman study on reduced flavin in purple intermediate of flavoenzyme Use of [4-carbonyl-^{18}O]-enriched flavin *J Biochem* **124**, 200–208
15 Nishina, Y , Sato, K., Hazekawa, I , and Shiga, K. (1995) Structural modulation of 2-enoyl-CoA bound to reduced acyl-CoA dehydrogenases A resonance Raman study of a catalytic intermediate *J Biochem* **117**, 800–808
16. Friedrich, H B and Person, W (1966) Infrared spectra of charge-transfer complexes. VI Theory *J Chem. Phys.* **44**, 2161–2170
17 Shiga, K., Nishina, Y , Horiike, K., Tojo, H , Watari, H , and Yamano, T (1980) On the existence of quasi D-amino acid oxidase in hog kidney extract *Med J Osaka Univ.* **30**, 71–78
18 Shiga, K., Nishina, Y , Horiike, K., Tojo, H , Yamano, T , and Watari, H (1982) A new material for flavoprotein researches Purification and properties of hog kidney quasi D-amino acid oxidase in *Flavins and Flavoproteins* (Massey, V and Williams, C H , Jr , eds) pp. 188–191, Elsevier North Holland, New York
19 Tojo, H., Horiike, K., Shiga, K., Nishina, Y , Miura, R , Watari, H , and Yamano, T (1982) Thermodynamic characterization of hog kidney D-amino acid oxidase apoenzyme in concentrated guanidine hydrochloride solution Preferential interaction with the solvent components and the molecular weight of monomer unit *J Biochem* **92**, 1741–1752
20 Miyake, Y , Abe, T , and Yamano, T (1971) Substrate induced dimerization of D-amino acid oxidase. *J. Biochem.* **70**, 719–722
21 Massey, V and Nishino, T (1980) D-Amino acid oxidase containing 7,8-dichloro-FAD instead of FAD in *Flavins and Flavoproteins* (Yagi, K. and Yamano, T , eds) pp 1–11, Japan Scientific Society Press, Tokyo
22 Cavallini, D , Ricci, G , Federici, G., Costa, M , Pensa, B , Matarese, R.M , and Achilli, M (1982) The oxidation of sulfur-containing amino acids by L-amino acid oxidase in *Structure and Function Relationships in Biochemical Systems* (Bossa, F , Chianone, E , Finazzi-Agr, A., and Strom, R , eds) pp 359–374, Plenum Press, New York
23 Busch, H , Nair, P.V , Frank, M , and Martin, W R (1958) Comparative pharmacological effects of a number of β-halogenated pyruvic acid. *J. Pharmacol. Exp Ther* **123**, 48–53
24. Yagi, K., Okamura, K., Naoi, M., Takai, A., and Kotaki, A. (1969) Reaction of D-amino acid oxidase with D-lysine *J. Biochem.* **66**, 581–589
25 Chang, Y F , Charles, A.K., and Tilkin, R.B. (1982) Assay of Δ^1-piperideine-2-carboxylate and synthesis of L-[^{14}C]pipecolate from DL-[^{14}C]pipecolate *Anal Biochem.* **125**, 376–385
26. Kuhn, R , Weygand, F , and Möller, E.F (1943) Über einen Antagonisten des Lactoflavins. *Ber Dtsch. Chem. Ges.* **76**, 1044–1051
27 Frisch, M.J., Trucks, G.W., Schlegel, H.B., Scuseria, G E , Robb, M.A , Cheeseman, J.R , Zakrewski, V G., Montgomery, J.A., Startman, R E , Burant, J C., Dapprich, S , Millan, J.M , Daniels, A.D , Kudin, K.N , Strain, M.C , Farkas, O , Tomasi, J , Barone, V , Cossi, M., Cammi, R., Mennucci, B , Pomelli, C ,

Adamo, C., Clifford, S., Ochterski, J., Petersson, A., Ayala, P.Y., Cui, Q., Morokuma, K., Malick, D.K., Rabuck, A.D., Raghavachari, K., Foresman, J.B., Cioslowski, J., Ortiz, J.V., Stefanov, B.B., Liu, G., Liashenko, A., Piskorz, P., Komaromi, I., Gomperts, R., Martin, R.L., Fox, D.J., Keith, T., Al-Laham, M.A., Peng, C.Y., Nanayakkara, A., Gonzalez, C., Challacombe, M., Gill, P.M., Johnson, B.G., Chen, W., Wong, M.W., Andres, J.L., Head-Gordon, M., Replogle, E.S., and Pople, J.A. (1998) *Gaussian 98*, Gaussian, Inc., Pittsburgh, PA, USA

28 Foresman, J.B. and Frisch, A. (1996) *Exploring Chemistry with Electronic Structure Methods*, 2nd ed., Gaussian, Inc., Pittsburg, PA, USA

29 Ricci, G., Nardini, M., Caccuri, A.M., and Federici, G. (1983) Interaction between 1,4-thiazine derivatives and D-amino-acid oxidase *Biochim. Biophys. Acta* **748**, 40–47

30 Nishina, Y., Sato, K., and Shiga, K. (1991) Isomerization of Δ^1-piperideine-2-carboxylate to Δ^2-piperideine-2-carboxylate on complexation with flavoprotein D-amino acid oxidase *J. Biochem* **109**, 705–710

31 Hazekawa, I., Nishina, Y., Sato, K., Shichiri, M., Miura, R., and Shiga, K. (1997) A Raman study on the C(4)=O stretching mode of flavins in flavoenzymes. Hydrogen bonding at the C(4)=O moiety *J. Biochem* **121**, 1147–1154

32 Dollish, F.R., Fateley, W.G., and Bentley, F.F. (1974) *Characteristic Raman Frequencies of Organic Compounds*, pp. 105–120, Wiley, New York

33 Nishina, Y., Tojo, H., and Shiga, K. (1988) Resonance Raman spectra of anionic semiquinoid form of a flavoenzyme, D-amino acid oxidase *J. Biochem* **104**, 227–231

34 Nishina, Y., Sato, K., Miura, R., and Shiga, K. (1995) Structures of charge-transfer complexes of flavoenzyme D-amino acid oxidase. A study by resonance Raman spectroscopy and extended Huckel molecular orbital method *J. Biochem* **118**, 614–620

35. Nishina, Y., Tojo, H., and Shiga, K. (1986) Complex formation between reduced D-amino acid oxidase and pyridine carboxylates *J. Biochem* **99**, 673–680

36 Nishina, Y., Tojo, H., Ushijima, H., and Shiga, K. (1987) Kinetic and equilibrium studies on the interaction of reduced flavoprotein D-amino acid oxidase with pyridine carboxylates. *J. Biochem.* **102**, 327–332

37 Massey, V. and Ganther, H. (1965) On the interpretation of the absorption spectra of flavoproteins with special reference to D-amino acid oxidase *Biochemistry* **4**, 1161–1173

38. Kakitani, H., Kakitani, T., Rodman, H., and Honig, B. (1983) Correlation of vibrational frequencies with absorption maxima in polyenes, rhodopsin, bacteriorhodopsin, and retinal analogues *J. Phys. Chem* **87**, 3620–3628

39 Baasov, T., Friedman, N., and Sheves, M. (1987) Factors affecting the C=N stretching in protonated retinal Schiff base a model study for bacteriorhodopsin and visual pigments. *Biochemistry* **26**, 3210–3217

40 Walter, T.J. and Braiman, M.S. (1994) Anion-protein interactions during halorhodopsin pumping· halide binding at the protonated Schiff base *Biochemistry* **33**, 1724–1733

41 Mulliken, R.S. and Person, W.B. (1969) *Molecular Complexes*, Wiley-Interscience, New York, London, Sydney, Toronto

42 Nishina, Y., Kitagawa, T., Shiga, K., Horiike, K., Matsumura, Y., Watari, H., and Yamano, T. (1978) Resonance Raman spectra of riboflavin and its derivatives in the bound state with egg riboflavin binding proteins. *J. Biochem* **84**, 925–932

43 Schopfer, L.M. and Morris, M.D. (1980) Resonance Raman spectra of flavin derivatives containing chemical modifications in positions 7 and 8 of isoalloxazine ring. *Biochemistry* **19**, 4932–4935